

Supplementary Information

for

Microchannel deformations due to solvent-induced PDMS swelling

Rémi Dangla

LadHyX and department of Mechanics, Ecole Polytechnique, CNRS 91128 Palaiseau Cedex, France

François Gallaire

*Institut de Génie Mécanique, Faculté des Sciences et Techniques de l'Ingénieur,
Ecole Polytechnique Fédérale de Lausanne, Switzerland*

Charles N. Baroud*

LadHyX and department of Mechanics, Ecole Polytechnique, CNRS 91128 Palaiseau Cedex, France

(Dated: May 21, 2010)

I. TRANSIENT EXPANSION OF A SWELLING PDMS SHEET

Here, we detail the calculations for determining the swelling characteristics of a solvent from the deformations it induces on a PDMS sheet. The swelling coefficient S_∞ and the diffusion coefficient D are obtained by comparing the observed time evolution of the length $L(t)$ of a PDMS sheet immersed in a bath of the solvent to a theoretical model. It is closely related to the method of sorption mass measurements described by J. Crank [1], which relies on the time evolution of the mass of the sheet. The method requires a precise prediction of the transient swelling geometry of the polymer sheet. To this end, we solve the coupled problems of solvent diffusion and induced mechanical strain. First, we compute the diffusion of the swelling solvent in the initial geometry, which we then deform by evaluating the local swelling expansion.

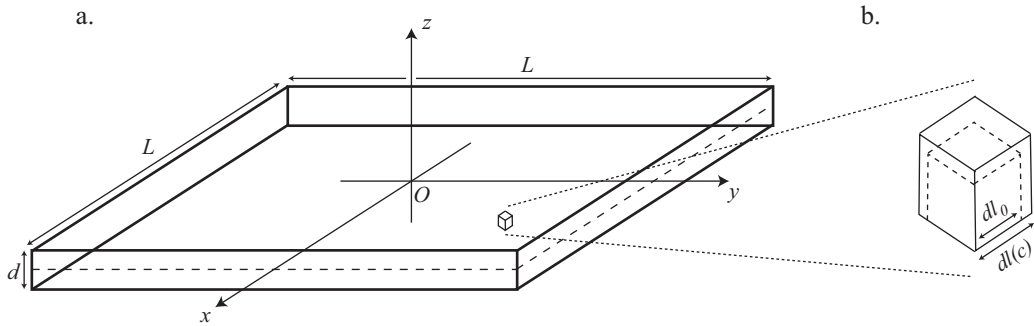


FIG. 1. **a.** Sketch of the thin square PDMS sheet and definition of the reference frame ($Oxyz$). **b.** Illustration of the local swelling expansion of a stress-free infinitesimal cube due to a solvent concentration c .

In the following derivations, we consider a square plane sheet of height d small compared to its width L ($d \ll L$). The center O of the coordinate system is taken as the center of symmetry of the sheet. The (x, y) -directions are along then in-plane directions while the z -direction is along the transverse direction, as sketched on Fig. 1.a.

A. Solvent diffusion and local swelling ratio s

The diffusion process of the solvent is characterized by a concentration at saturation c_∞ and a diffusion coefficient D . In this model, we assume that D is independent of the solvent concentration, such that $c(\vec{x}, t)$ verifies the classical diffusion equation with saturated boundary conditions

$$\frac{\partial c}{\partial t} = D_s \vec{\nabla}^2 c(\vec{x}, t) \text{ in } \Omega, \quad c = c_\infty \text{ on } \partial\Omega, \quad (1)$$

where Ω and $\partial\Omega$ are the inner volume and the boundaries of the sheet, respectively.

The local swelling induced by the solvent is quantified through the local swelling ratio $s(\vec{x}, t)$. It is defined as the ratio between the size $dl(c)$ of a stress-free, infinitesimal cube at the concentration $c(\vec{x}, t)$ over its dry size dl_0 (see Fig. 1.b).

Next, we make an analogy with linear thermoelasticity. In the same way that thermal strain is assumed to be proportional to the temperature field T [2], we make the assumption that the local swelling ratio $s(\vec{x}, t)$ varies linearly with the concentration field of the solvent $c(\vec{x}, t)$. In addition, it saturates at S_∞ , yielding

$$s(\vec{x}, t) - 1 = \frac{c(\vec{x}, t)}{c_\infty} (S_\infty - 1). \quad (2)$$

Therefore, the swelling ratio $s(\vec{x}, t)$ also verifies the classical diffusion equation with saturated boundary conditions :

$$\frac{\partial s(\vec{x}, t)}{\partial t} = D \vec{\nabla}^2 s(\vec{x}, t) \text{ in } \Omega, \quad s = S_\infty \text{ on } \partial\Omega. \quad (3)$$

For a thin plane sheet, there is a scale separation between in-plane (x, y) and transverse z coordinates. This allows us to model the diffusion process as a one dimensional problem in the transverse direction and to treat the

concentration field as a function of z and t only. In this case, the solutions for equations (1) and (3) can be found in textbooks [1]. They are

$$\begin{aligned} \frac{c(z,t)}{c_\infty} &= 1 - \frac{4}{\pi} \sum_{n=0}^{\infty} \frac{(-1)^n}{2n+1} \cos \frac{(2n+1)\pi z}{d} \exp \left(-\frac{D(2n+1)^2 \pi^2 t}{d^2} \right), \\ \frac{s(z,t) - 1}{S_\infty - 1} &= 1 - \frac{4}{\pi} \sum_{n=0}^{\infty} \frac{(-1)^n}{2n+1} \cos \frac{(2n+1)\pi z}{d} \exp \left(-\frac{D(2n+1)^2 \pi^2 t}{d^2} \right). \end{aligned} \quad (4)$$

Plots of this concentration field $c(z,t)$ are shown on Fig. 2.a for different values of time t .

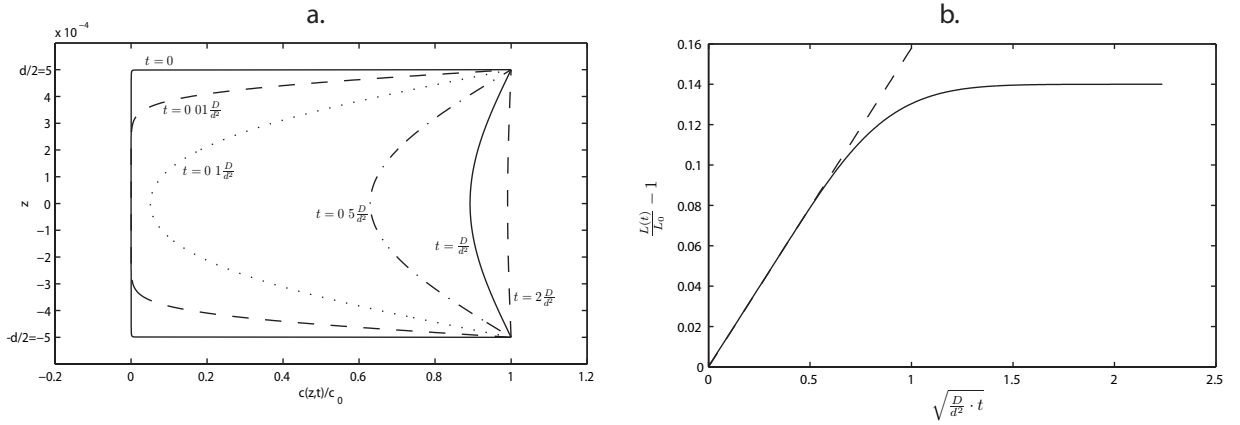


FIG. 2. **a.** Concentration profiles $c(z,t)$ plotted using equation (4) for different times $t = [0, 0.01, 0.1, 0.5, 1, 2] \cdot D/d^2$. **b.** Plots of the overall strain $L(t)/L_0 - 1$ for $S_\infty = 1.14$ as a function of $\sqrt{d^2 \cdot t/D}$, the square root of the nondimensional time: using the exact solution from equation (15) (solid line) and using the initial time approximation from equation (16) (dashed line).

B. The swollen geometry

To estimate the transient swelling geometry, we recall the analogy with linear thermoelasticity and rely on the classical models that relate a given strain to mechanical stresses [2]. In our case, the concentration profile $c(z,t)$ imposed by diffusion induces a local swelling ratio $s(\vec{x},t)$, which can be expressed as a swelling strain: $\underline{\underline{\epsilon}}^s = (s(z,t) - 1)\underline{\underline{\mathbb{1}}}$. This strain tensor is not geometrically compatible: there does not exist any physical displacement field $\vec{\xi}(\vec{x},t)$ that creates such a strain. In particular, it violates the second compatibility equation

$$\frac{\partial^2 \epsilon_{yy}^s}{\partial z^2} + \frac{\partial^2 \epsilon_{zz}^s}{\partial y^2} \neq 2 \frac{\partial^2 \epsilon_{yz}^s}{\partial y \partial z}. \quad (5)$$

As a result, the observed strain $\underline{\underline{\epsilon}}$ has to be different from the natural swelling strain $\underline{\underline{\epsilon}}^s$ and it induces internal mechanical stresses $\underline{\underline{\sigma}}$ according to the Hook relation [2]:

$$\underline{\underline{\sigma}} = 2\mu(\underline{\underline{\epsilon}} - \underline{\underline{\epsilon}}^s) + \lambda Tr(\underline{\underline{\epsilon}} - \underline{\underline{\epsilon}}^s)\underline{\underline{\mathbb{1}}}. \quad (6)$$

We recall the thin sheet limit ($d \ll L$) to assume problem invariance in the (x,y) plane. When used along with the compatibility equations, this limits the strain tensor to the form

$$\underline{\underline{\epsilon}} = \begin{pmatrix} \gamma(t) & 0 & 0 \\ 0 & \gamma(t) & 0 \\ 0 & 0 & f(z,t) \end{pmatrix}, \quad (7)$$

where $\gamma(t)$ and $f(z,t)$ are the unknowns to be determined.

Plugging this strain into equation (6), the stress tensor becomes

$$\begin{aligned}\sigma_{xx} &= \sigma_{yy} = 2\mu[\gamma(t) - (s(z, t) - 1)] + \lambda[2(\gamma(t) - (s(z, t) - 1)) + (f(z, t) - (s(z, t) - 1))] , \\ \sigma_{zz} &= 2\mu[f(z, t) - (s(z, t) - 1)] + \lambda[2(\gamma(t) - (s(z, t) - 1)) + (f(z, t) - (s(z, t) - 1))]\end{aligned}\quad (8)$$

and shear components are zero.

At this point, we assume that the solid responds instantaneously to the variations of swelling strain induced by the diffusion process. Hence, the stress tensor must verify the equation of statics $\vec{\text{div}}\underline{\underline{\sigma}} = 0$ with unconstrained boundary conditions. This yields

$$\begin{aligned}\langle \sigma_{xx} \rangle_z &= \langle \sigma_{yy} \rangle_z = 0 , \\ \sigma_{zz} &= 0 , \forall z ,\end{aligned}\quad (9)$$

where the $\langle \cdot \rangle_z$ operator is the mean in the z -direction. At each time t , these equations lead to a coupled linear system in terms of $f(z)$ and γ

$$\begin{aligned}2(\lambda + \mu)(\gamma - \langle s - 1 \rangle_z) + \lambda(\langle f \rangle_z - \langle s - 1 \rangle_z) &= 0 , \\ (2\mu + \lambda)(f(z) - (s - 1)) + 2\lambda(\gamma - (s - 1)) &= 0 ,\end{aligned}\quad (10)$$

which has a unique set of solutions

$$\begin{aligned}\gamma(t) &= \langle s(z, t) - 1 \rangle_z , \\ f(z, t) &= \frac{3\lambda + 2\mu}{\lambda + 2\mu} (s(z, t) - 1) - \frac{2\lambda}{2\lambda + \mu} \langle s(z, t) - 1 \rangle_z .\end{aligned}\quad (11)$$

These results can be further simplified in the case of PDMS because it is a nearly incompressible elastic solid, i.e. a material for which $\mu \ll \lambda$. Hence, the observed deformation is

$$\begin{aligned}\xi_x(x, y, z, t) &= \langle s(z, t) - 1 \rangle_z \cdot x , \\ \xi_y(x, y, z, t) &= \langle s(z, t) - 1 \rangle_z \cdot y , \\ \xi_z(x, y, z, t) &= 3 \int_0^z (s(z, t) - 1) dz - 2 \langle s(z, t) - 1 \rangle_z \cdot z .\end{aligned}\quad (12)$$

In practice, the measurable quantities in an experiment are the overall thickness $d(t)$ and length $L(t)$ of the sheet. They are

$$\begin{aligned}d(t) &= d_0 + 2\xi_z(d_0/2, t) = \langle s(z, t) \rangle_z \cdot d_0 , \\ L(t) &= L_0 + 2\xi_x(L_0/2, t) = \langle s(z, t) \rangle_z \cdot L_0 .\end{aligned}\quad (13)$$

In the end, we find that the inhomogeneous swelling strain $s(z, t) - 1$ induces a homothetic transformation on the overall geometry of the swollen sheet: the length and thickness evolve as if the sheet is homogeneously swollen by the solvent at a concentration $\langle c(z, t) \rangle_z$. Thereby, the overall length of a square swelling sheet is unambiguously defined by

$$\frac{L(t)}{L_0} = \langle s(z, t) \rangle_z .\quad (14)$$

C. Combining diffusion and deformations

The swelling ratio $s(z, t)$ is given by the diffusion of a swelling solvent into the immersed sheet. Therefore, the transient length of the swelling sheet $L(t)$ is found by combining the main results from the two previous subsection, in Eq. (4) and Eq. (14), to yield

$$\frac{L(t)}{L_0} - 1 = (S_\infty - 1) \cdot \left(1 - \frac{4}{\pi^2} \sum_{n=0}^{\infty} \frac{1}{(2n+1)^2} \exp\left(-\frac{D(2n+1)^2\pi^2 t}{d^2}\right) \right) .\quad (15)$$

For initial times, this expression simplifies [1] to

$$\frac{L(t)}{L_0} - 1 = (S_\infty - 1) \frac{2}{d} \sqrt{\frac{Dt}{\pi}} .\quad (16)$$

A comparative plot between the full solution (15) and the initial time approximation (16) is shown on Fig. 2.b, revealing a good agreement until $t \approx d^2/D$.

II. HEIGHT PROFILES FOR CHANNELS OF VARIOUS WIDTH

- [1] J. Crank, *The Mathematics of Diffusion*, Oxford Science Publications, 1975.
[2] R. B. Hetnarski and M. R. Eslami, *Thermal Stresses - Advanced Theory and Applications*, Springer, 2008.

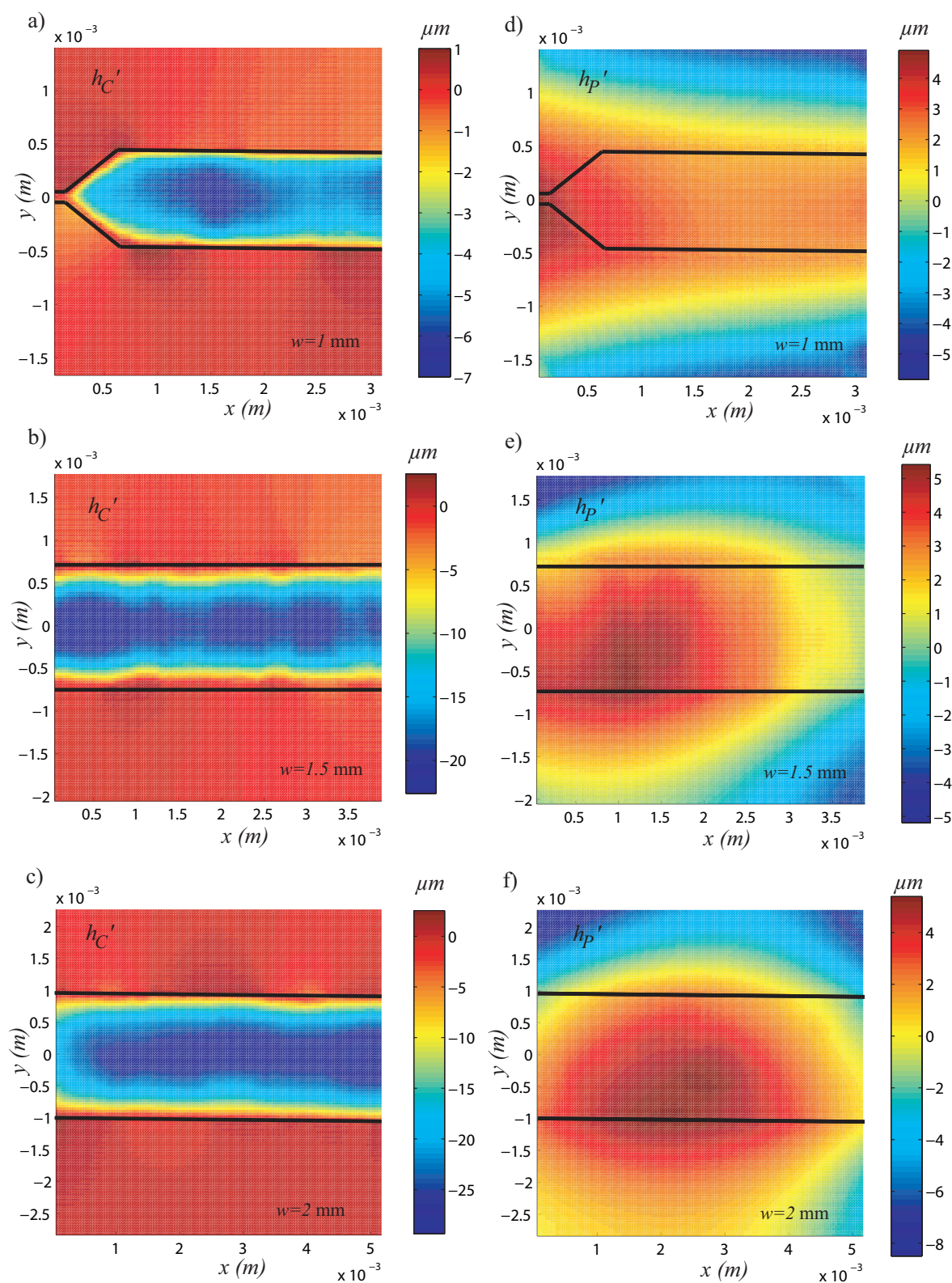


FIG. 3. Deformations of microchannels measured by the Synthetic Schlieren method. The position of the channel is outlined by solid lines. a-c) Height profiles h'_C of the roof of the test section swollen by hexadecane for channels of width 1 mm, 1.5 mm and 2 mm respectively. d-f) Height profiles h'_P of the top surface of the PDMS block swollen by hexadecane for the same channels of width 1 mm, 1.5 mm and 2 mm respectively.